A model of self-thinning through local competition

F. R. ADLER*

Departments of Mathematics and Biology, University of Utah, Salt Lake City, UT 84112

ABSTRACT   Explanations of self-thinning in plant populations have focused on plant shape and packing. A dynamic model based on the structure of local interactions successfully reproduces the pattern and can be approximated to identify key parameters and relationships. The approach generates testable new explanations for differences between species and populations, unifies self-thinning with other patterns in plant population dynamics, and indicates why organisms other than plants can follow the law.

Ecological patterns tend to be obscured by noise. Those that stand out must derive from robust structural or dynamical principles. One such pattern is the $-3/2$ self-thinning law for plant populations (1, 2). As individuals in a competing population of even-aged plants grow, their mean biomass, B, increases and their number, n, decreases, with the trajectory plotting $\log(B)$ against $\log(n)$ often approaching a line with slope near $-3/2$, or

$$\log(B) = c - 1.5 \log(n) \qquad [1]$$

for a wide range of species (1, 2). Some sample forestry data are shown in Fig. 1. The graphs plot the log mean size against the log number of trees over time, starting in the lower right corner with a large number of plants of small size, and moving up and to the left as the number of plants decline and the plants grow.

Deviations from a slope of $-3/2$ are common (4–7). Existing theories derive self-thinning from packing arguments that lack individual mechanisms and explain variation around the expected relation by making specific assumptions about packing (4–11). I here derive the relation and the deviations from a dynamic model of local resource competition that provides a testable individual level mechanism underpinning these packing arguments. This model suggests an alternative way to analyze data, unifies the law with the development of size hierarchies in plant population dynamics, and indicates why populations of algae (12) and animals (13) might have similar dynamics.

A General Model of Local Competition

The decrease in numbers during self-thinning results from mortality that preferentially strikes plants that have fallen behind in growth (1, 2, 5–7). The basic differential equation describing growth is

$$\frac{dy_i}{dt} = r_i y_i, \qquad [2]$$

where y_i is the mass of plant i and r_i is its relative growth rate. In a competing population, r_i depends on local resource availability, which depends in turn on the size of and distance to neighbors, in addition to other abiotic and biotic sources of heterogeneity.

In the model, the relative growth rate r_i is built from a local competition function that describes the per unit mass effect of a plant of mass y at distance d. We assume that plant j takes resources from plant i at distance d_{ij} according to

$$\text{effect} = y_j^{k_1} g(y_j^{k_2}, d_{ij}).$$

The "local competition function" g must be increasing in y, decreasing in d, and have scaling $g(y, 0) = 1$. The exponent k_1 scales maximum resource absorption as a function of mass, and k_2 scales how effect decreases with distance (Fig. 2). A large value of k_1 exaggerates the local effect of large plants and describes one form of asymmetric competition (14, 15) (Fig. 2 *Lower Left*). A large value of k_2 stretches the spatial extent of effects of large plants and produces another form of asymmetry (Fig. 2 *Lower Right*). These differences correspond to differences in the resource exploitation profiles of plants of different sizes, and link this argument with arguments based on shape (8).

The total competitive effect $\gamma_i(t)$ at time t on plant i is the sum

$$\gamma_i(t) = \sum_{j \neq i} y_j^{k_1} g(y_j^{k_2}, d_{ij}). \qquad [3]$$

If r_i is proportional to the fraction of local absorption controlled by plant i, growth obeys

$$\frac{dy_i}{dt} = \frac{y_i^{k_1}}{y_i^{k_1} + \gamma_i} y_i, \qquad [4]$$

where the maximum relative growth rate has been scaled to 1. When γ_i is small relative to y_i, the plant grows exponentially near its maximum rate. When γ_i is large relative to y_i, growth nearly stops. Simulations of the model generate an increasingly skewed size hierarchy. The model is a generalization of earlier models that used particular forms of the local competition function (16–18).

Effective Number and the Size Hierarchy

Because the model does not include mortality, I recast the self-thinning process in terms of the "effective number" of plants. The effective number N gives less weight to small plants that can modify the self-thinning relation (19) or are not counted (3). Formally, N is the reciprocal of the probability that two units of mass chosen at random from the population come from the same plant, or

$$N = \frac{1}{\sum_{i=1}^{n} p_i^2} = \frac{\left(\sum_{i=1}^{n} y_i \right)^2}{\sum_{i=1}^{n} y_i^2} = \frac{y_T^2}{M_2}, \qquad [5]$$

where p_i is the fraction of mass in plant i, y_T is the total biomass, and M_2 is the second moment of the biomass distribution. The effective number N is less than or equal to the census number n, with equality only when all plants have the same size. The

*e-mail: adler@math.utah.edu.

Population Biology: Adler

Proc. Natl. Acad. Sci. USA 93 (1996)   9981
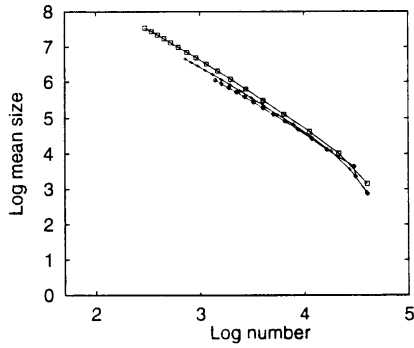
FIG. 1.   Self-thinning curves for three stands of *Pseudotsuga men-ziesii* (3): stand 85 (diamonds), stand 105 (plus signs), and stand 145 (squares). Growth in each stand moves up and to the left, with values measured every 5 years starting from ages ranging from 20 to 30 years. The slopes are approximately −1.68 (4). Log number is normalized to match the values in Fig. 3.

effective mean biomass M is the total biomass divided by the effective number, or $M = y_T/N = M_2/y_T$.

Writing effective number and mean size in terms of the moments of the distribution, the self-thinning relation $M \propto N^{-3/2}$ translates to $M_2 \propto y_T^4$. In terms of effective number, the −3/2 self-thinning law encodes a particular power function relation between moments of the mass distribution. In general, $M_2 \propto y_T^p$ corresponds to

$$M \propto N^{-\frac{p-1}{p-2}}. \qquad [6]$$

$p > 2$ indicates development of a size hierarchy, $p < 2$ indicates a decrease in the size hierarchy, and $p = 2$ indicates equal growth with no development of a size hierarchy.

Simulation Results

The particular value $p = 4$ arises from the dynamics of local competition. Fig. 3 plots $\log(M)$ against $\log(N)$ generated by simulations using exponential, Gaussian, fractional, and step function versions of the local competition function, the last
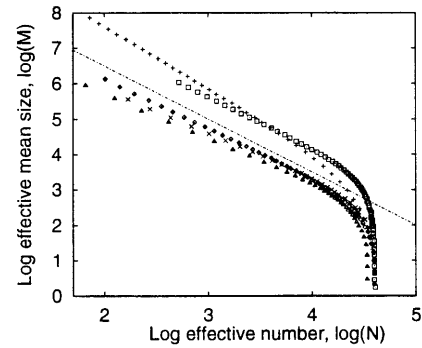
FIG. 3.   Simulations of self-thinning (Eq. **4**) compared with a line of slope −3/2 with $k_1 = 1$, using an exponential form $g(y, d) = e^{-\alpha d/y}$ with $\alpha = 50$ (diamonds), a Gaussian form $g(y, d) = e^{-\alpha d^2/y}$ with $\alpha = 750$ (plus signs), a fractional form $g(y, d) = 1/(1 + \alpha d/y)$ with $\alpha = 400$ (squares), and a step function $g(y, d) = 1$ if $\alpha d/y > 1$ and $g(y, d) = 0$ if $\alpha d/y < 1$ with $\alpha = 50$ (×). Values of α were chosen to roughly match the mean initial competitive effects. Each dot indicates an elapsed time of 0.3. Plants ($n = 100$) of initial biomass 1.0 were scattered randomly with uniform density on a 2 by 2 torus, except for one simulation using the exponential local competition function with $\alpha = 50$, but with initial variability generated by placing 100 plants in a rectangular grid with initial sizes chosen uniformly from the range 0.5 to 1.5 (triangles). The pattern persists when both forms of variability are combined.

corresponding to neighborhood models (17, 20). In each case, the slope approaches the value −3/2, although the Gaussian form produces a steeper slope for reasons explained below. Even with initial conditions of very different forms (21), simulations are similar. These robust results describe a characteristic pattern of amplification of variability created by local interaction. Globally averaged competition, in which all plants compete for the same pool of resources, creates a very different pattern.

Fig. 4 plots the minimum slope achieved (the minimum ratio of the logarithmic derivatives of M and N) during simulations of self-thinning as a function of k_1 and k_2. The slope of the self-thinning relation becomes less steep with larger values of k_1 and k_2, corresponding to a more rapid development of the size hierarchy with more asymmetric competition.
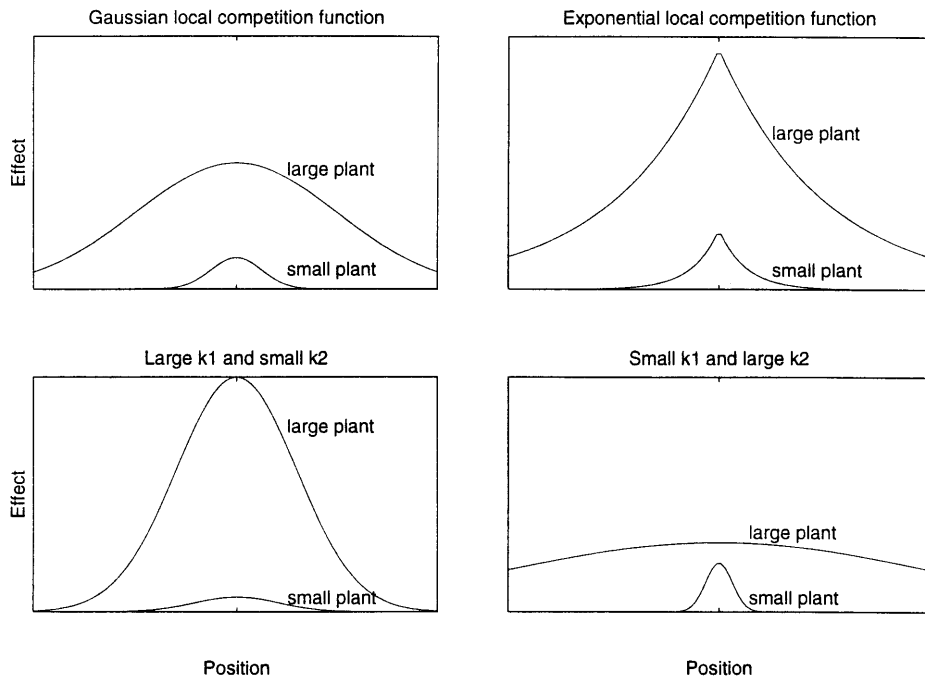
FIG. 2.   Comparison of effects of small and large plants with different local competition functions and different values of k_1 and k_2.
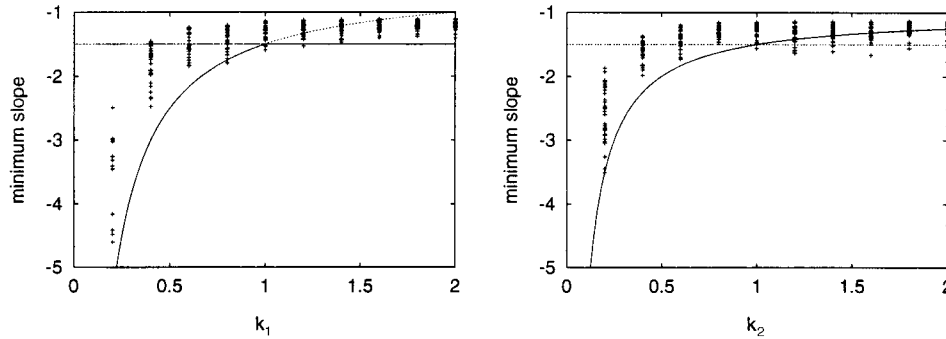
FIG. 4.   (*Left*) The minimum slope achieved (the minimum ratio of the logarithmic derivatives of M and N) during simulations of self-thinning as a function of k_1 when $k_2 = 1$. (*Right*) The minimum slope achieved as a function of k_2 when $k_1 = 1$. The curve is the theoretical value given in Eq. **9** (see text), where the dotted portion (*Left*) indicates the region where the approximation is not strictly justified. Simulations use the exponential local competition function and combinations of $n = 50$, $n = 100$, and $n = 200$ with $\alpha = 10$, $\alpha = 50$, and $\alpha = 100$. Use of the minimum slope rather than fitting the straight portion of the curve overestimates the slope. Simulations tend to produce lower slopes for larger values of n unless plant growth slows at larger sizes.

Other simulations show that the dynamics of effective and census number match if a plant dies when its relative growth rate drops below a threshold value (about 0.06 for the parameters used here), but that self-thinning is more rapid for higher thresholds.

Approximation of the Dynamics

The robust behavior can be explained by approximating the equations. First, we estimate the competitive effect $\gamma_i(t)$ as a function of the mean biomass $\bar{y}(t)$ and the initial competitive effect $\gamma_i(0)$. Simulations show that log competitive effect depends approximately linearly on the log initial competitive effect, or that

$$\ln(\gamma_i(t)) \approx a(t) \ln(\gamma_i(0)) + b(t). \qquad [7]$$

We can approximate the mean and variance of $\gamma_i(t)$ as functions of the mean biomass $\bar{y}(t)$ (Appendix A) finding that

$$\gamma_i(t) \approx \beta h_E \bar{y}(t)^{k_1+2k_2} e^{-\frac{E_0\theta}{\bar{y}(t)^{k_2}}} \gamma_i(0)^{\frac{\theta}{\bar{y}(t)^{k_2}}} \qquad [8]$$

in two dimensions, where the parameters β, h_E, E_0, and θ are functions of the density and the local competition function. Each factor of k_2 is multiplied by $D/2$ in D dimensions.

Substituting this expression for $\gamma_i(t)$ into the full system of local competition equations (Eq. **4**) produces a highly nonlinear system, simplified in that the growth of each plant is coupled only to the mean biomass. Simulations of this approximation match simulations of the full model over time (Fig. 5), and predict quantitatively how final size depends on $\log(\gamma_i(0))$.

The simplest equation retaining dependence on $\gamma_i(0)$ and a function of $\bar{y}(t)$ matching the dominant term in equation 8 sets $\gamma_i(t) = \gamma_i(0)\bar{y}(t)^{k_1+2k_2}$. With much further approximation (Appendix B), we can derive a simplified system for which the self-thinning slope can be computed explicitly as

$$\text{self-thinning slope} = -\frac{1}{k_1} - \frac{1}{2k_2} \qquad [9]$$

(Fig. 4). When $k_1 = k_2 = 1$, shape is preserved (Fig. 2), competition is proportional to biomass, and the slope is $-3/2$, matching the results of packing arguments. In D dimensions, $2k_2$ is replaced by Dk_2, changing the slope to a smaller value of $(D + 1)/D$ (22). In contrast to the exponential local competition function, the Gaussian local competition function $g(y,d) = e^{-\alpha d^2/y}$ depends on $d/\sqrt{y}$, so that $k_2 = 0.5$. The expected slope is then -2, steeper than $-3/2$ (Fig. 3). Self-thinning thus depends on the shape of the resource depletion profile (Fig. 2) in addition to the degree of competitive asymmetry.

Discussion

These results derive self-thinning and deviations from the $-3/2$ law from an individual based model of resource-mediated growth. Large values of the scaling exponents k_1 and k_2 produce self-thinning slopes close to -1, and small values produce large slopes, potentially explaining the wide distribution of observed slopes (4–7). Because the model explicitly follows individual plant sizes rather than population level averages (8, 11), it makes specific predictions about the connection between the spatial pattern and the size hierarchy (5–7, 23–25). The approximations show that robust statistical principles underlie the population level patterns that emerge from this individual behavior.

Testing can begin with direct measurement of the local competition function and the exponents k_1 and k_2, from which appropriate measures of local crowding can be derived. Studies that have failed to identify local competition with standard spatial statistics (26) might succeed by using the initial competitive effect $\log(\gamma_i(0))$ estimated in this way. The model might also apply to self-thinning in algae and animals (13) if "local" competition is interpreted as similarity of resource use rather than proximity. In addition, the specific predictions regarding the success of given plants as a function of local competition makes possible prediction of the evolution of local interaction strategies.
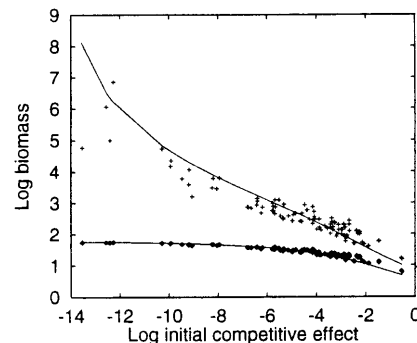
FIG. 5.   Comparison of a simulation with the approximation (Eq. **8**) at two times. The log biomass $\ln(y_i)$ is plotted against the log initial competitive effect $\ln(\gamma_i(0))$ at the two times 1.5 and 15.9 using the exponential local competition function $g(y, d) = e^{-\alpha d/y}$ with $\alpha = 50$.

Population Biology: Adler

Proc. Natl. Acad. Sci. USA 93 (1996)   9983

Appendix A

To find the slope and intercept of Eq. **7**, we approximate the mean and variance of the γ's using the "zero-correlation" approximation (27) and some properties of random distributions of points. Suppose plants are arrayed in space according to a Poisson process with density β. γ_i can be estimated by setting $y_j = \bar{y}$ for every $j \neq i$, where $\bar{y}$ is the mean size in the population, ignoring the fact that the sizes of nearby plants might be correlated.

Each of our candidate local competition functions (Fig. 3) can be written in the form $g(y^{k_2}, d) = h\,(d/y^{k_2})$ for some function h. Because γ_i is the sum of the effects of other plants, its expected value $\mu(t)$ can be computed by integrating over all distances. Changing variables to $s = r/\bar{y}^{k_2}$,

$$\mu(t) = \int_0^\infty 2\pi r \beta \bar{y}^{k_1} h\left(\frac{r}{\bar{y}^{k_2}}\right) dr$$

$$= \beta \bar{y}^{k_1+2k_2} \int_0^\infty 2\pi s h(s) ds = \beta \bar{y}^{k_1+2k_2} h_E . \qquad [10]$$

Similarly, when the locations of plants are independent, the variance $\sigma^2(t)$ is

$$\sigma^2(t) = \int_0^\infty 2\pi r \beta \bar{y}^{2k_1} h^2\left(\frac{r}{\bar{y}^{k_2}}\right) dr$$

$$= \beta \bar{y}^{2k_1+2k_2} \int_0^\infty 2\pi s h^2(s) ds = \beta \bar{y}^{2k_1+2k_2} h_V . \qquad [11]$$

The values h_E and h_V *depend only on the function h*, so that μ and σ depend on $\bar{y}$ only through the power functions.

At time t, $\gamma_i(t) = \mu(t) + b_i(t)\sigma(t)$ for some set of values $b_i(t)$. The set of $b_i(t)$ must have mean 0 and variance 1. If $\sigma(t) \ll \mu(t)$ as in simulations, $\ln(\gamma_i(t)) \approx \ln(\mu(t)) + b_i(t)\sigma(t)/\mu(t)$. Therefore, $E(\ln(\gamma)) \approx \ln(\mu(t))$ and $\mathrm{Var}(\ln(\gamma)) \approx \sigma^2(t)/\mu^2(t)$. Denote the expectation and variance of $\ln(\gamma)$ by E_0 and V_0 at time $t = 0$. The expectation and variance of Eq. **7** are $a(t)\,E_0 + b(t)$ and $a^2(t)V_0$, respectively. Solving for $a(t)$ and $b(t)$, we find

$$a(t) = \frac{\sigma(t)}{\mu(t)\sqrt{V_0}} \qquad [12]$$

$$b(t) = \ln(\mu(t)) - \frac{\sigma(t)E_0}{\mu(t)\sqrt{V_0}} . \qquad [13]$$

These values were substituted into Eq. **7** to derive Eq. **8**.

Appendix B

We begin by deriving a piecewise linear approximation of Eq. **4**. Set $x_i = y_i^{k_1}$. Rewriting the definition of γ_i (Eq. **3**) with the function h as in Appendix A and changing gives

$$\dot{x}_i = k_1 \frac{x_i}{x_i + \gamma_i} x_i$$

$$\gamma_i = \sum_{j \neq i} x_j h\left(\frac{d_{ij}}{x_j^{\frac{k_2}{k_1}}}\right).$$

The formula for γ_i has the form of Eq. **3** with k_1 replaced by 1 and k_2 replaced by k_2/k_1. Suppose that γ_i can be approxi-

mated by $\gamma_i(0)\bar{x}^{\bar{k}}$ where $\bar{k} = 1 + 2k_2/k_1$ (Appendix A). We approximate again to derive the equation

$$\dot{x}_i = \begin{cases} x_i - \gamma_i(0)\bar{x}^{\bar{k}} & \text{if positive} \\ 0 & \text{otherwise} \end{cases} \qquad [14]$$

by scaling out the multiplicative factor k_1 and expanding growth in a first order Taylor series truncated to remain positive.

Until the growth stops, x_i follows a linear equation. During this time, Eq. **14** has solution $x_i(t) = e^t\,(1 - \gamma_i(0)\,X(t))$where $X(t) = \int_0^t e^{-s}\bar{x}^{\bar{k}}ds$. To fully solve, we need to find the time T when the plant stops growing. This time is a function only of the initial crowding $\gamma_i(0)$, so we write $T(\gamma_i(0))$ as the solution of

$$e^t(1 - \gamma_i(0)X(t)) - \gamma_i(0)\bar{x}^{\bar{k}} = 0.$$

Using the definition of X, this can be rewritten as $1 - \gamma_i(0)X(t) = \gamma_i(0)\dot{X}(t)$.

To get rid of the index i, we write $\gamma_i(0)$ as $T^{-1}(t_i)$, where T^{-1} is well-defined because the derivative of x_i in Eq. **14** is a monotonically decreasing function of $\gamma_i(0)$). Therefore, $1 - T^{-1}(t)X(t) = T^{-1}(t)\dot{X}(t)$, which has solution $X(t) = e^{-t}\int_0^t e^s/T^{-1}(s)ds$ with initial condition $X(0) = 0$.

We can now derive a reduced system of differential equations for the moments of the distribution. Define $\dot{Z}(t) = \int_0^t e^s/T^{-1}(s)ds$. Then

$$\dot{Z}(t) = \frac{e^t}{T^{-1}(t)} = Z + e^t\dot{X} = Z + \bar{x}^{\bar{k}}. \qquad [15]$$

To find a differential equation for $\bar{x}$, let $f(\gamma)$ denote the probability density function of the initial $\gamma_i(0)$ with maximum possible value γ_m. Then

$$\bar{x}(t) = \int_0^{T^{-1}(t)} e^t(1 - \gamma X(t))f(\gamma)d\gamma + \int_{T^{-1}(t)}^{\gamma_m} e^{T(\gamma)}$$

$$\times \ (1 - \gamma X(T(\gamma)))f(\gamma)d\gamma. \qquad [16]$$

Differentiating and simplifying,

$$\dot{x}(t) = e^t \int_0^{T^{-1}(t)} f(\gamma)d\gamma - \dot{Z} \int_0^{T^{-1}(t)} \gamma f(\gamma)d\gamma. \qquad [17]$$

This equation and Eq. **15** form a closed system because every appearance of $T^{-1}(t)$ and $\dot{Z}$ can be replaced with functions of Z and $\bar{x}$.

These equations have asymptotically exponential solutions when the density f has the form $f(\gamma) = \gamma^{1/q-1}/q$ for a positive value of q and $0 \leq \gamma \leq 1$. Suppose that $\bar{x}$ increases exponentially with parameter α (i.e., $\bar{x} \propto e^{\alpha t}$). Then, from Eq. **15**, we have that $T^{-1}(t)$ increases exponentially with parameter $1 - \alpha\bar{k}$. But Eq. **17** also implies that $\bar{x}$ increases exponentially proportional to $e^t T^{-1}(t)^{(1/q)}$. These two expressions give an equation for α, which can be solved to give $\alpha = (1 + q)/(q + \bar{k})$.

To check the self-thinning relation expressed in Eq. **6**, we must find the first two moments of the distribution of the actual sizes y_i. By writing equations similar to Eq. **16**, and substituting in the exponential forms for X and T^{-1}, we find that $\bar{y}$ increases exponentially with parameter $1/k_1 + (1 - \alpha\bar{k})/q$ and M_2 increases exponentially with parameter $2/k_1 + (1 - \alpha\bar{k})/q$. The power p relating the growth of the first and second moments is the ratio of these exponents. Transforming into the slope (Eq. **6**), we find

$$\text{slope} = -\frac{1}{k_1} - \frac{1+q}{2k_2}.$$

The form of the approximation **8** indicates that the initial competitive effect $\gamma_i(0)$ is raised to a power that approaches 0 as plants grow. The value $q = 0$ therefore provides the best approximation, and is used in Eq. **9**.

1. Yoda, K., Kira, T., Ogawa, H. & Hozumi, K. (1963) *J. Biol. Osaka City Univ.* **14,** 107–129.
2. White, J. & Harper, J. L. (1970) *J. Ecol.* **58,** 467–485.
3. Curtis, R. O., Clendenen, G. W., Reukoma, D. L. & DeMars, D. J. (1982) *Yield Tables for Managed Stands of Coast Douglas-Fir* (Department of Agriculture, Washington, DC), Volume PNW-135 of Gen. Tech. Rep.
4. Lonsdale, W. M. (1990) *Ecology* **71,** 1373–1388.
5. Westoby, M. (1984) *Adv. Ecol. Res.* **14,** 167–225.
6. Weller, D. E. (1987) *Ecol. Monog.* **57,** 23–43.
7. Zeide, B. (1987) *For. Sci. (Sofia)* **33,** 517–537.
8. Weller, D. E. (1987) *Ecology* **68,** 813–821.
9. Norberg, R. A. (1988) *Am. Nat.* **131,** 220–256.
10. Clark, J. S. (1990) *J. Ecol.* **78,** 275–299.
11. Osawa, A. & Allen, R. B. (1993) *Ecology* **74,** 1020–1032.
12. Cousens, R. & Hutchings, M. J. (1983) *Nature (London)* **301,** 240–241.
13. Latto, J. (1994) *Oikos* **69,** 531–534.
14. Thomas, S. C. & Weiner, J. (1989) *Oecologia* **80,** 349–355.
15. Weiner, J. (1990) *Trends Ecol. Evol.* **5,** 360–364.
16. Weiner, J. (1984) *J. Ecol.* **72,** 183–196.
17. Pacala, S. W. & Weiner, J. (1991) *J. Theor. Biol.* **149,** 165–179.
18. Benjamin, L. R. & Hardwick, R. C. (1986) *Ann. Bot.* **58,** 757–778.
19. West, P. W. & Borough, C. J. (1983) *Ann. Bot.* **52,** 149–158.
20. Czaran, T. & Bartha, S. (1992) *Trends Ecol. Evol.* **7,** 38–42.
21. Miller, T. E. & Weiner, J. (1989) *Ecology* **70,** 1188–1191.
22. Furnas, R. E. (1981) Ph.D. thesis (Cornell Univ., Ithaca).
23. Levin, S. A., Levin, J. E. & Paine, R. T. (1977) *Condor* **79,** 395.
24. Kenkel, N. C. (1988) *Ecology* **69,** 1017–1024.
25. Kohyama, T. (1994) *J. Plant Res.* **107,** 107–116.
26. Kenkel, N. C., Hoskins, J. A. & Hoskins, W. D. (1989) *Can. J. Bot.* **67,** 2630–2635.
27. Gurney, W. S. C. & Nisbet, R. M. (1978) *Am. Nat.* **112,** 1075–1090.